in the vapor region, respectively; ', ", relating to the parameters of the liquid and of the vapor in the state of saturation.

LITERATURE CITED

1. V. A. Maiorov and L. L. Vasil'ev, "The structure of an evaporating stream inside heated porous metal," Inzh.-Fiz. Zh., 41, No. 6, 965-969 (1981).
2. V. A. Maiorov and L. L. Vasil'ev, "Analytical model of biphase cooling of a porous fuel element," in: Intensification of the Processes of Energy and Mass Transfer in Porous Media at Low Temperatures, Institute of Heat and Mass Transfer (ITMO), Minsk (1975), pp. 140-148.
3. V. A. Maiorov and L. L. Vasil'ev, "The temperature state of the system of evaporative cooling of a porous fuel element," in: Low-Temperature Heat Pipes and Porous Heat Exchangers, Institute of Heat and Mass Transfer (ITMO), Minsk (1977), pp. 3-11.
4. V. A. Maiorov, "Flow and heat exchange of a single-phase heat-transfer agent in porous cermet materials," Teploenergetika, No. 1, 64-70 (1978).
5. V. A. Maiorov, "Intensification of heat exchange in the evaporation of a stream in a channel with porous, highly heat conducting filler," Promyshlennaya Teplotekh., 3, No. 4, 22-28 (1981).
6. V. A. Maiorov and L. L. Vasil'ev, "Nucleation of gas and vapor bubbles upon motion of a liquid in porous metals," Inzh.-Fiz. Zh., 42, No. 4, 533-539 (1982).

HYDRODYNAMICS OF RIVULET FLOW ON A VERTICAL SURFACE

I. M. Fedotkin, G. A. Mel'nichuk,
F. F. Koval', and E. V. Klimkin

UDC 536.248.5

The flow of rivulets on a vertical surface is investigated theoretically and experimentally.

Liquid flow in the form of individual rivulets occurs upon the breakup of a liquid film. Such a regime can occur, for example, in heat-transfer devices where heat is transferred through evaporation—condensation of the heat-transfer agent [1] and in the emergency film cooling of nuclear reactors. It is closely connected with the formation of dry patches on a heated surface [2]. As investigations showed [1, 2], in such a regime rather intense heat removal from the surface occurs without causing a sharp increase in its temperature.

The majority of the research has been devoted to problems of the hydrodynamics and stability of liquid film flow or the stability of rivulet flow [3-6].

The hydrodynamics of rivulet flow has still been inadequately studied. In [7], for example, the connection between the flow rate in a rivulet and its width was obtained on the basis of a solution of the Navier—Stokes equation for rivulet flow, and it was compared with experiment and showed only qualitative agreement. The problem of describing rivulet flow is divided into two parts: the first is to describe the shape of the surface of the rivulet; the second is to find the velocity distribution in the rivulet.

In accordance with [7], we use the following physical model of rivulet flow. The shape of the rivulet is determined only by surface tension; we neglect gravity. The rivulet is represented in the form of a segment of a circle which does not vary during the entire flow. All the physical properties of the liquid remain constant. The rivulet moves uniformly in one direction under the action of gravity. We take the flow as fully developed and steady. Shear stresses at the interface are absent.

The adopted physical model and coordinate system are shown in Fig. 1. Under the adopted assumptions the Navier—Stokes equations take the form

---

Kiev Polytechnic Institute. Translated from Inzhenerno-Fizicheskii Zhurnal, Vol. 46, No. 1, pp. 14-20, January, 1984, Original article submitted August 10, 1982.

0022-0841/84/4601-0009$08.50

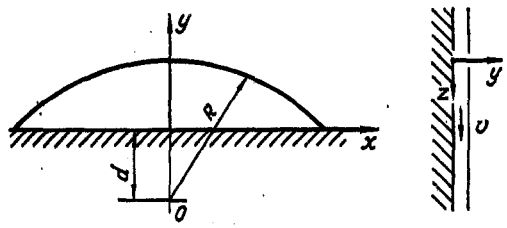

Fig. 1. Diagram of rivulet flow.

$$\frac{dP}{dx} = 0, \quad \frac{dP}{dy} = 0, \tag{1}$$

$$\frac{dP}{dz} = -\rho g, \tag{2}$$

$$\frac{\partial^2 v}{\partial x^2} + \frac{\partial^2 v}{\partial y^2} = -\frac{g}{\nu}. \tag{3}$$

The boundary conditions will be

$$v = 0 \text{ at } y = 0, \tag{4}$$

$$\frac{\partial v}{\partial x} = 0 \text{ at } x = 0. \tag{5}$$

The condition of the absence of shear stresses at the interface can be written as

$$\frac{\partial v}{\partial n} = 0. \tag{6}$$

To find the liquid flow rate in a rivulet with a given width and wetting angle one must solve Eq. (3) with the boundary conditions (4)-(6):

$$Q = \int_{-l/2}^{l/2} \int_{0}^{y} v(x;\ y)\, dxdy. \tag{7}$$

Equations (3)-(7) will have the dimensionless form

$$\frac{\partial^2 V}{\partial X^2} + \frac{\partial^2 V}{\partial Y^2} = -1, \tag{8}$$

$$V = 0 \text{ at } Y = 0, \tag{9}$$

$$\frac{\partial V}{\partial X} = 0 \text{ at } X = 0, \tag{10}$$

$$\frac{\partial V}{\partial N} = 0 \text{ (at the interface)}, \tag{11}$$

$$G = \int_{-P/2}^{+P/2} \int_{0}^{Y} V(X;\ Y)\, dXdY, \tag{12}$$

where $X = x/a$; $Y = y/a$; $N = n/a$; $V = \mu v/\sigma$; $G = g\mu\rho Q/\sigma^2$.

In [7] Eq. (8) was solved approximately and on the basis of the assumption that

$$\frac{\partial^2 V}{\partial X^2} \ll \frac{\partial^2 V}{\partial Y^2}, \tag{13}$$

while under the boundary condition

$$\frac{\partial^2 V}{\partial Y^2} = 0 \text{ (at the interface)} \tag{14}$$

TABLE 1. Values of the Coefficients of the Polynomials P_1 and P_2 for the Four Coordinate Functions

Coordinate functions	P_1	P_2
X^2	$6{,}53058021 \cdot 10^{-2}$	$-9{,}6425284 \cdot 10^{-1}$
X^4Y^2	$1{,}5102875 \cdot 10^{-1}$	$1{,}1447087 \cdot 10^{-1}$
X^6Y^3	$2{,}5531338 \cdot 10^{-1}$	$6{,}153968 \cdot 10^{-1}$
X^8Y^4	$1{,}5945653 \cdot 10^{-1}$	3,9812201

the equation had the form

$$\frac{\partial^2 V}{\partial Y^2} + 1 = 0. \tag{15}$$

However, such an assumption [7] is valid only for a plane rivulet, such as occurs for a small wetting angle. This assumption can serve as a first approximation, since the law of variation of the velocity along the x coordinate actually is parabolic.

The method of R functions [8] is used to solve the Poisson differential equation (8) with the mixed boundary conditions (9)-(11). The most important feature of R functions is their "kinship" with functions of logic algebra, which results in the existence of additional properties of R functions permitting the introduction of the methods of discrete mathematics into the classical methods of continuous analysis. This permits the analytical allowance for the geometrical information (the shape of the boundary of the region and subregions, the interfaces between the media, etc.) contained in the statement of the boundary-value problems. One can construct bundles of functions [8] satisfying the given boundary and initial conditions and containing the exact solution of the problem or a sufficiently good approximation of it. An element of a bundle of functions is formalized using the concept of the structure of the solution of the boundary-value problem [9]. The structure of the solution allowing for the a priori conditions must be determined within the region. This leads to the need to extend into the region the functions and operators assigned at the boundary.

For this purpose we introduce special operators with coefficients dependent on the shape of the region. In particular, the operators D_n and T_n perform extension of the corresponding n-th-order derivatives normally and tangentially.

The structure of the solution of the problem (8)-(11) has the form

$$V = \omega_1 P_1 - \omega\,[D^{(2)}(\omega_1 P_1 + \omega_2 P_2)], \tag{16}$$

where $\omega = \omega_1 \wedge_0 \omega_2 = \omega_1 + \omega_2 - \sqrt{\omega_1^2 + \omega_2^2}$; here $\wedge_0$ is an R conjunction; $\omega_1 = Y$ and $\omega_2 = [X^2 + (Y + d)^{(2)} - R^2]\ 1/2R = 0$ is the equation for the boundary of the rivulet;

$$D^{(2)}(\omega_1 P_1) = (\nabla\omega_1,\ \nabla(\omega_1 P_1)) = \frac{\partial\omega_2}{\partial X}\frac{\partial}{\partial X}(\omega_1 P_1) + \frac{\partial\omega_2}{\partial Y}\frac{\partial}{\partial Y}(\omega_1 P_1)$$

is a linear differential operator while

$$P_1 = \sum_{i=1}^{n_1'}\sum_{i=1}^{n_2'} C_{ij} X^{2i} Y^j;\quad P_2 = \sum_{k=1}^{n_1''}\sum_{s=1}^{n_2''} C_{ks} X^{2k} Y^s$$

are power-law polynomials (Chebyshev and Legendre polynomials can be used). The function (16) satisfies the boundary conditions (9)-(11).

The unknown quantities in (16) are the coefficients C_{ij} and C_{ks}. They can be determined by one of the variational methods (we use Ricci's method). The conditions of a minimum of the functional

$$J(\omega) = \iint_\Omega \left[\left(\frac{\partial V}{\partial X}\right)^2 + \left(\frac{\partial V}{\partial Y}\right)^2 - 2V\right] dX dY \tag{17}$$

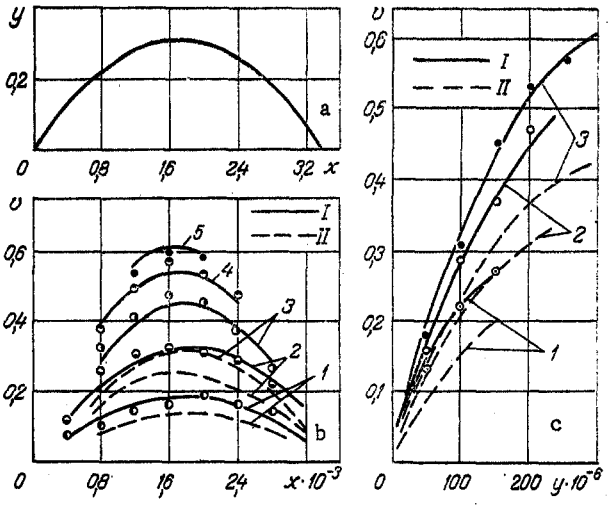

Fig. 2. Comparison of the theoretical and experimental velocity distributions in a rivulet: a) shape of a rivulet (experiment); y, x, mm; b) distribution of velocities v (m/sec) over the x coordinate (m); I) experiment; II) theory: 1) $y = 50 \cdot 10^{-6}$ m; 2) $100 \cdot 10^{-6}$; 3) $150 \cdot 10^{-6}$; 4) $200 \cdot 10^{-6}$; c) distribution of velocities v (m/sec) over the y coordinate (m): I) experiment; II) theory: 1) $x = 2.8 \cdot 10^{-3}$ m; 2) $2.4 \cdot 10^{-3}$; 3) $2.0 \cdot 10^{-3}$.

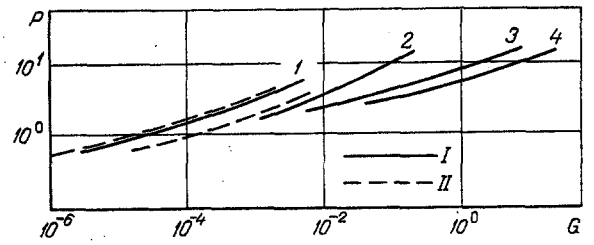

Fig. 3. Dependence of the dimensionless rivulet width P on the dimensionless flow rate G: I) calculation; II) from [7]: 1) $\Theta = 10°$; 2) 20; 3) 30; 4) 40.

are

$$\frac{\partial J}{\partial C_{ij}} = 0, \quad \frac{\partial J}{\partial C_{ks}} = 0 \quad (i = \overline{1, n_1'};\ j = \overline{1, n_2'};\ k = \overline{1, n_1''};\ s = \overline{1, n_2''}).$$

They lead to the solution of the system of linear algebraic equations, by solving which we find C_{ij} and C_{ks}.

The problem was solved on a BÉSM-6 computer. The integrals (elements of the Green's matrix) were calculated by Gauss's method while the system of algebraic equations was solved by the rotation method. The differentiation of the coordinate functions was automated and carried out exactly. The machine time expended was from 2 to 12 min, depending on the number of coordinate functions (n_1 = 12, 16, 18) and the number of integration nodes (n_2 = 10, 20, 40).

The values of the coefficients to the four coordinate functions are presented in Table 1.

The velocity distribution in rivulets was investigated experimentally using a laser Doppler velocity meter [10] by the scheme presented in [11]. The laser radiation passed through a light divider and then was focused on the investigated point using a microscope objective.

Light scattered by particles (d = 1-3 μm) introduced into the liquid was received by a photomultiplier, while the electrical signal from the photomultiplier was sent to an amplifier and then to a spectrum analyzer, from which the Doppler frequency of the scattered light, appearing as a result of the motion of the particles, was determined.

The velocity of liquid motion (since the particle density equals the liquid density and they are entrained by all the pulsations of the liquid) was determined from the equation

$$V = \frac{f_d \lambda}{2\sin\frac{\alpha}{2}}, \tag{18}$$

where λ is the wavelength of the laser radiation; α is the angle of intersection of the laser beams.

The working section consisted of a plastic plate 25 × 600 mm in size. A porous baked metal insert, through which liquid was supplied to the plate from a constant-level tank, was mounted in the upper part of the plate flush with it. The liquid was circulated with a centrifugal pump. The flow rate was measured volumetrically in the range of 11-255 ml/min. The plate was set up vertically on a special micrometer table, allowing us to move it in two mutually perpendicular directions in the horizontal plane.

The smallest movement permitted by the table in the horizontal plane was 10 μm. The table also provided for vertical movement of the plate. At the start of a test the point of intersection of the beams was brought to the inner plane of the plate not occupied by the rivulet. The appearance of noise on the screen of the spectrum analyzer indicated the presence of the point of intersection on the inner wall. As the plate was moved in the horizontal direction, when the point of intersection of the beams touched the edge of the stream there was a decrease in the noise level on the screen of the spectrum analyzer. This was due to the very small thickness of the stream, less than the resolving power in the transverse direction, which greatly altered the scattering indicatrix. As the plate moved further in the horizontal direction the recovery of the scattering indicatrix, i.e., the recovery of the noise level, took place. When the opposite edge of the stream reached the point of intersection of the rays the noise level decreased. The difference in the readings on the dial of the table gave the width of the stream. In each test the stream width was divided into no less than five cross sections, in each of which the velocity distribution was taken. The surface of the rivulet was determined from the dropout of the signal on the screen of the spectrum analyzer.

The velocity profiles were measured with a constant flow rate and a constant rivulet width. The rivulet width and the velocity profile were measured in several cross sections along the stream and compiled into one series of data.

The shape of a rivulet is shown in Fig. 2a and the velocity profiles in transverse (Fig. 2b) and longitudinal (Fig. 2c) cross sections. The difference between the calculated and experimental values does not exceed 30%.

The difference between the experimental and theoretical results is evidently due to the presence of waves on the rivulet surface. According to [7], the transition to wavy flow occurs at Reynolds numbers Re = 20-40. Here we note that waves on a rivulet surface have a lesser influence on the width of the rivulet and more on the wetting angle. Therefore, the rivulet shape realized on the average approaches a segment of a circle. The theoretical dependence of the dimensionless flow rate on the dimensionless width of a rivulet, calculated for different wetting angles, is presented in Fig. 3. The theoretical dependence of [7] is plotted in the same figure. A comparison of these two dependences shows that they coincide at small flow rates and small wetting angles. With an increase in flow rate and wetting angle, however, a deviation toward an increase in the authors' data is observed. This is due to the fact that, in contrast to [7], the two-dimensional flow problem was solved.

The velocity distribution in each cross section of a rivulet is described by an equation analogous to that presented in [11], the general form of which is

$$V_z = Ay - By^2, \tag{19}$$

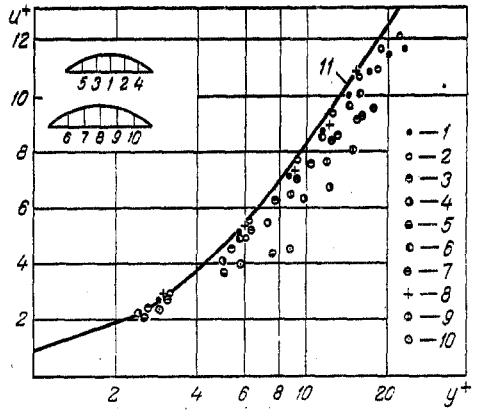

Fig. 4. Dependence $u^+ = f(y^+)$ for different rivulet cross sections: 1-5) Re = 279; 6-10) 1649; 11) from [11].

where A and B are empirical coefficients.

In [11] Eq. (19) describes the flow of a thin liquid film in the same range of Reynolds numbers as in the present investigation. This indicates that flow along the Y coordinate in a rivulet in the given range of Reynolds numbers takes place independently of the transverse coordinate X.

In Fig. 4 we present the dependence of the dimensionless velocity on the dimensionless coordinate y^+ by analogy with [11]. The experimental points for the two extreme Reynolds numbers are generalized satisfactorily by the dependence presented in [11]:

$$y^+ = u^+ + 0{,}111\,(\exp 0{,}34u^+ - 1). \tag{20}$$

NOTATION

x, y, z, Cartesian coordinates; n, normal to the surface; P, pressure; v, velocity of rivulet flow; l, rivulet width; ρ, liquid density; σ, surface tension; g, free-fall acceleration; ν, kinematic viscosity; Q, liquid flow rate in rivulet; f_d, Doppler frequency; $\sqrt{\sigma/\rho g} = a$, capillary constant; $\mathrm{Re} = 4Q/l\nu$, Reynolds number; Λ_0, R conjunction; R, radius of a segment of a circle; d, distance from the center of the circle to the middle of the chord of the segment, particle diameter; Ω, region of integration; $v_* = \sqrt{\tau_w/\rho}$, dynamic velocity; τ_w, wall shear stress; $y^+ = vy/\nu$, dimensionless coordinate; $u^+ = v/v_*$, dimensionless velocity; Θ, wetting angle.

LITERATURE CITED

1. F. E. Andros, "The two-phase close thermosyphon: an experimental study," Proceedings, Condensed Papers, Two-Phase Flow and Heat-Transfer Symposium, Workshop, Fort Lauderdale, Fla., October (1976), pp. 247-250.
2. G. F. Hewitt and N. S. Hall-Taylor, Annular Two-Phase Flow, Pergamon Press, Oxford—New York (1970).
3. D. E. Hartly and F. Murgatroyd, "Criteria for the break up of thin liquid layers flowing isothermally over a solid surface," Int. J. Heat Mass Transfer, 7, No. 9, 1003-1015 (1964).
4. N. Zuber and F. W. Staub, "Stability of dry patches forming in liquid film flowing over heated surface," Int. J. Heat Mass Transfer, 9, No. 1, 145-152 (1961).
5. T. Hobler and J. Czaika, "Minimal wetting of a flat surface," Chem. Stosow., 2B, No. 1, 169-174 (1968).
6. J. Mikielewicz and J. R. Moszynski, "Minimum thickness of liquid film flowing vertically down a solid surface," Int. J. Heat Mass Transfer, 19, No. 7, 771-776 (1976).
7. G. D. Towell and L. B. Rothfeld, "Hydrodynamics of rivulet flow," AIChE J., No. 9, 972-980 (1966).
8. V. L. Rvachev and A. P. Slesarenko, Logic Algebra and Integral Transformations in Boundary-Value Problems [in Russian], Naukova Dumka, Kiev (1976).
9. V. L. Rvachev, Methods of Logic Algebra in Mathematical Physics [in Russian], Naukova Dumka, Kiev (1974).
10. B. S. Rinkevichyus, Laser Anemometry [in Russian], Énergiya, Moscow (1978).
11. M. G. Semena and G. A. Mel'nichuk, "Velocity distribution in a descending liquid film," Izv. Vyssh. Uchebn. Zaved., Energ., No. 5, 143-147 (1978).